BROADBAND GSC BEAMFORMER WITH SPATIAL AND TEMPORAL DECORRELATION

Choo Leng Koh[1], *Soydan Redif*[2] *and Stephan Weiss*[3]

[1] Communications Research Group, School of ECS, University of Southampton, UK
[2] Engineering Faculty, Near East University, Nikosia, Turkey
[3] Centre for Excellence in Signal and Image Processing, Dept. of EEE, University of Strathclyde, Glasgow, UK
augustine.koh@eads.net, sredif@neu.edu.tr, stephan.weiss@eee.strath.ac.uk

ABSTRACT

Broadband adaptive beamforming algorithms based on the least mean square (LMS) family are known to exhibit slow convergence, if the input is correlated. In this paper, we will utilised a recently proposed broadband eigenvalue decomposition method to provide strong spatial decorrelation, while at the same time reduces the subspace in which the beamforming algorithm operates. Additional temporal decorrelation is gained by operating the beamformer in oversampled filter banks. Hybrid structures which combine both spatial and temporal decorrelation demonstrate to provide faster convergence speed than the normalised LMS algorithm or either of the decorrelation approach on its own.

1. INTRODUCTION

For a number of applications, particularly in acoustics, beamformers are required to operate across a wide bandwidth at a considerable spatial and spectral resolution. This results in systems with a large number of sensors, M, followed by tap-delay lines (TDLs) of considerable length L. If adaptive solutions to this beamforming problem are sought,. then the dimensionality of the beamforming problem generally prohibits the use of computationally intensive but fast converging algorithms such as the recursive least squares (RLS) family [1] or the Newton method [2]. In contrast, approaches with low computational cost such as those based on the LMS-type adaptive filter [3] are prone to slow convergence particularly when the number of coefficients is high and the input signal correlated due to highly structured interference.

Best convergence conditions are realised for LMS-type adaptive algorithms, if the input to the adaptive filter is decorrelated and all modes of convergence have equal power [3, 4]. In [4] this is achieved by preprocessing the TDLs with a Karhunen-Loeve transform (KLT) — or suboptimally by a number of data-independent transforms such as the DFT, DCT, or DST — which decorrelates the input vector to the adaptive filter. An additional power normalisation stage is generally required to realise fast convergence, but may hamper steady-state performance due to noise amplification.

Translating [4] to beamforming and multichannel filtering means that the KLT is applied across all channels and lags spanned in the TDLs. Applying the KLT to the spatial dimension only works for narrowband beamforming, but neglects correlation across successive lags arising from convolutive mixing, which extends over both spatial and temporal dimensions. Therefore after convolutive mixing, previously independent signals are not just spatially correlated at the same time instance but also over a range of lag values.

This paper proposes the use of a recently introduced broadband eigenvalue decomposition (BEVD) [5] to perform strong decorrelation, which removes correlation between any pair of signals for all lag values, in order to improve the convergence behaviour of an LMS broadband adaptive beamformer. As an example, we apply this technique to a generalised sidelobe canceller, which is briefly reviewed in Sec. 2, together with its input covariance matrix and traditional decorrelation approaches. Sec. 3 introduces strong decorrelation by means of a BEVD to the input of the adaptive filter. Strong spatial decorrelation is complemented by temporal prewhitening using an oversampled subband approach [6, 7] in Sec. 4, resulting in two structures, whose performances are compared to a number of benchmarks in Sec. 5. Finally, conclusions are drawn in Sec. 6.

2. GSC BEAMFORMER

A linearly constrained minimum variance (LCMV) beamformer performs the minimisation of variance of an output signal with respect to some spatial and spectral constraints [8]. The LCMV problem can be implemented alternatively by the GSC technique [9], which performs project the data onto an unconstrained subspace where standard optimisation methods such as RLS or LMS can be readily applied. The projection is performed via a quiescent vector $\mathbf{w}_c$ and a blocking matrix $\mathbf{C}_a$, who are constructed from the beamformer's constraint equation. The aim of the quiescent vector is to isolate the signal of interest (SOI) as best as possible, while the blocking matrix removes any SOI components, such that the subsequent adaptive filter operates in an adaptive noise cancellation architecture [3].

2.1 Simplified GSC Structure

For a broadband SOI impinging onto a linear array from broadside, the blocking matrix can be simplified by the cascaded columns of differencing (CCD) method [9]. In a simplest case, CCD provides a quiescent vector

$$\mathbf{w}_c = \frac{1}{M}[1\ 1\ \cdots\ 1]^T \quad \in \mathbb{R}^M . \tag{1}$$

and block matrix that subtracts adjacent sensor signals using

$$\mathbf{C}_a = \begin{bmatrix} 1 & -1 & & & \mathbf{0} \\ & \ddots & \ddots & & \\ & & \ddots & \ddots & \\ \mathbf{0} & & & 1 & -1 \end{bmatrix} \quad \in \mathbb{C}^{(M-1)\times M} . \tag{2}$$

The simplification is based on $\mathbf{C}_a$ only being applied to the spatial component of the data. However, with sensor array data collected in $\mathbf{x}[n]$, it can be easily the verified that

$$\mathbf{u}_{\mathrm{S}}[n] = \mathbf{C}_a\mathbf{x}[n] \quad \in \mathbb{C}^{M-1} \,, \tag{3}$$

is free of SOI. The blocking matrix output $\mathbf{u}_{\mathrm{S}}[n] \in \mathbb{C}^M$ contains spatial data only, and need to be buffered in tap delay lines (TDLs) prior to being passed as $\mathbf{u}_{\mathrm{ST}}[n] \in \mathbb{C}^{(M-1)L}$ to the adaptive filter vector $\mathbf{w}_a \in \mathbb{C}^{(M-1)L}$ as shown on Fig. 1. The adaptive filter is optimised based on a suitable criterion applied to the error $e[n]$ which is obtained by subtracting the adaptive filter output from the quiescent signal $d[n]$.

2.2 Covariance Matrix

When optimising $\mathbf{w}_a$ based on LMS-type algorithms,the speed of convergence is influenced by the data covariance matrix

$$\mathbf{R}_{uu,\mathrm{ST}} = \mathscr{E}\left\{\mathbf{u}_{\mathrm{ST}}[n]\mathbf{u}_{\mathrm{ST}}^H[n]\right\} \,. \tag{4}$$

based on the input $\mathbf{u}_{\mathrm{ST}}[n]$ to the adaptive filter in Fig. 1. This covariance matrix can also be expressed as

$$\mathbf{R}_{uu,\mathrm{ST}} = \begin{bmatrix} \mathbf{R}_{uu,\mathrm{s}}[0] & \mathbf{R}_{uu,\mathrm{s}}[-1] & \dots & \mathbf{R}_{uu,\mathrm{s}}[-L+1] \\ \mathbf{R}_{uu,\mathrm{s}}[1] & \mathbf{R}_{uu,\mathrm{s}}[0] & \ddots & \vdots \\ \vdots & \ddots & \ddots & \mathbf{R}_{uu,\mathrm{s}}[-1] \\ \mathbf{R}_{uu,\mathrm{s}}[L-1] & \dots & \mathbf{R}_{uu,\mathrm{s}}[1] & \mathbf{R}_{uu,\mathrm{s}}[0] \end{bmatrix} \tag{5}$$

where

$$\mathbf{R}_{uu,\mathrm{S}}[\tau] = \mathscr{E}\left\{\mathbf{u}_{\mathrm{S}}[n]\mathbf{u}_{\mathrm{S}}^H[n-\tau]\right\} \,, \tag{6}$$

contains spatial covariance only, based on the blocking matrix output $\mathbf{u}_{\mathrm{S}}[n]$

$$\mathbf{u}_{\mathrm{S}}[n] = \begin{bmatrix} u_{s,0}[n] \\ u_{s,1}[n] \\ \vdots \\ u_{s,M-2}[n] \end{bmatrix} \tag{7}$$

as shown in Fig. 1.

2.3 Decorrelation

In order to decorrelate the input to the adaptive filter, the above covariance matrices need to be diagonalised. This can be obtained by a Karhunen-Loeve transform (KLT) based on either $\mathbf{R}_{uu,\mathrm{S}}[\tau]$ or $\mathbf{R}_{uu,\mathrm{ST}}[\tau]$. If a KLT is applied to the input of the TDL block in Fig. 1, then $\mathbf{R}_{uu,\mathrm{S}}[\tau]$ is diagonalised while for $\mathbf{R}_{uu,\mathrm{ST}}[\tau]$ only the block-diagonal elements

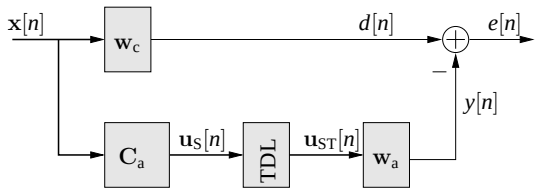

Figure 1: Generalised sidelobe canceller.

$\mathbf{R}_{uu,\mathrm{S}}[0]$ are diagonalised, while the remainder of the matrix remains non-sparse.

The application of the KLT is in general not sufficient in order to increase the convergence speed, since a power normalisation stage is also required in order to balance all modes of convergence [4].

[PERHAPS LEAVE OFF?]

3. GSC WITH STRONG SPATIAL DECORRELATION

This section outlines a method to achieve strong decorrelation of the data vector $\mathbf{u}_{\mathrm{S}}[n]$ acquired by the sensor array as shown in Fig. 1.

3.1 Broadband Eigenvalue Decomposition

In this paper, we use the broadband eigenvalue decomposition as defined in [5], which is the extension of the well known EVD to the case of a polynomial matrix, here

$$\mathbf{R}_{uu,\mathrm{S}}(z) = \sum_{\tau=-\infty}^{\infty} \mathbf{R}_{uu,\mathrm{S}}[\tau]z^{-\tau} \quad . \tag{8}$$

Note that $\mathbf{R}_{uu,\mathrm{S}}(z)$ is parahermitian, i.e. $\mathbf{R}_{uu,\mathrm{S}}(z) = \tilde{\mathbf{R}}_{uu,\mathrm{S}}(z)$ whereby $\tilde{(\cdot)}$ indicates the parahermitian operator, $\tilde{\mathbf{R}}_{uu,\mathrm{S}}(z) = \mathbf{R}_{uu,\mathrm{S}}^H(z^{-1})$. The BEVD of such a parahermitian matrix is given by

$$\mathbf{R}(z)_{uu,\mathrm{s}}(z) = \mathbf{U}(z)\Lambda(z)\tilde{\mathbf{U}}(z) \,, \tag{9}$$

where $\mathbf{U}(z)$ is paraunitary such that $\mathbf{U}(z)\tilde{\mathbf{U}}(z) = \mathbf{I}$ and $\Lambda(z)$ is a diagonal matrix

$$\Lambda(z) = \mathrm{diag}\{\Lambda_0(z), \Lambda_1(z), \dots \Lambda_{M-2}(z)\} \,. \tag{10}$$

Similar to the standard EVD, $\mathbf{U}(z)$ preserves the signal power, however, the "eigenvalues" $\Lambda_i(z)$, $i = 0 \cdots (M-2)$, are polynomials which are spectrally majorised, i.e. the power spectral densities $\Lambda_i(e^{j\Omega}) = \Lambda_i(z)|_{z=e^{j\Omega}}$ satisfy

$$\Lambda_0(e^{j\Omega}) \geq \Lambda_1(e^{j\Omega}) \geq \dots \geq \Lambda_{M-2}(e^{j\Omega}) \,, \quad \forall\Omega \,. \tag{11}$$

Spectral majorisation provides an ordering akin to the singular value decomposition, which removes ambiguity in the decomposition.

3.2 Sequential Best Rotation Algorithm

To calculated the BEVD for a given polynomial covariance matrix $\hat{\mathbf{R}}(z)$, the sequential best rotation algorithm using second order statistics (SBR2) is utilised as proposed in [5].

SBR2 is an iterative technique, which consists of a sequence of elementary steps involving a time shift in combination with a Givens rotation in order to eliminate the largest off-diagonal element of the remaining parahermitian matrix. The algorithms stops if off-diagonal elements have been suppressed below a specified threshold, or if a maximum number of iterations has been exceeded. The result for an estimated polynomial covariance matrix $\hat{\mathbf{R}}_{uu,\mathrm{s}}(z)$ is a decomposition

$$\mathbf{R}_{uu,\mathrm{s}}(z) = \mathbf{H}(z)\hat{\Lambda}(z)\tilde{\mathbf{H}}(z) \tag{12}$$

with a guaranteed paraunitary matrix $\mathbf{H}(z)$, and an approximately diagonalised and spectrally majorised $\hat{\Lambda}(z)$.

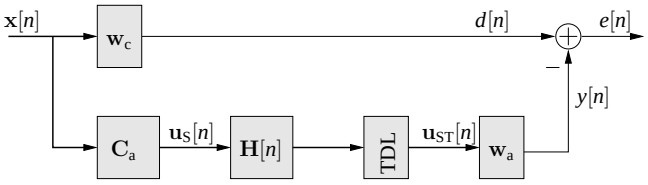

Figure 2: BEVD-based GSC with a paraunitary preprocessor $\mathbf{H}(z)$ to achieve a strong spatial decorrelation for the inputs to the adaptive filter $\mathbf{w}_a$.

3.3 Remaining Covariance Matrix

When applying the paraunitary matrix $\mathbf{H}(z) \bullet\!\!-\!\!\circ\, \mathbf{H}[n]$ to the array data $\mathbf{u}_S[n]$ in Fig. 2, the covariance matrix at the output of $\mathbf{H}[n]$ has been diagonalised and spectrally majorised according to (10). As a result, the input to the adaptive process, $u_{ST}[n]$, has the following associated covariance matrix,

$$\mathbf{R}_{uu,ST} = \begin{bmatrix} \hat{\Lambda}[0] & \hat{\Lambda}[-1] & \dots & \hat{\Lambda}[-L+1] \\ \hat{\Lambda}[1] & \hat{\Lambda}[0] & \ddots & \vdots \\ \vdots & \ddots & \ddots & \hat{\Lambda}[-1] \\ \hat{\Lambda}[L-1] & \dots & \hat{\Lambda}[1] & \hat{\Lambda}[0] \end{bmatrix} . \quad (13)$$

This matrix is not entirely diagonalised but has only $2L-1$ bands with non-sparse entries. Further, due to spectral majorisation, the outputs of $\mathbf{H}[n]$ will have decreasing power, and only a reduced number of broadband sources are considered, then only those outputs carrying power may be utilised for further processing, thus reducing the dimension of the data and subsequently the computation cost of beamforming algorithms.

However, if a GSC is operated on the output of $\mathbf{H}[n]$ as shown in Fig. 2, then temporal correlation remains as a potential source of slow convergence when using LMS-type algorithms. The next section will introduce a method to additionally reduce this temporal correlation.

4. GSC WITH SPATIO-TEMPORAL DECORRELATION

To perform additional temporal whitening for the BEVD-GSC beamformer depicted in Fig. 2, we here follow a subband approach based on oversampled filter banks [6].

4.1 Filter Bank-Based Temporal Decorrelation

Amongst a number of different subband adaptive structures, oversampled systems have been proven to perform very successfully [10, 11] and with a clearly defined bound for the minimum mean square error performance [7], which can be directly considered in the filter bank design [12]. The subband approach is based on separating the signal into K well-defined frequency bands such that only adjacent bands overlap, and decimated by a factor of $N < K$ such that aliasing in the subbands is kept to a minimum. The subband signals are correlated due to the redundancy introduced in oversampling, but can be processed independently with the MMSE limited by the alias level.

In order to reduce the filter bank complexity, oversampled modulated filter banks are used, which only require the

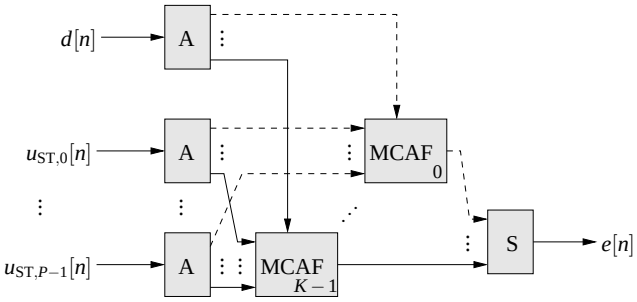

Figure 3: Multichannel adaptive filters (MCAF) operating in each of the K subbands created by $P+1$ analysis filter banks (A) and one synthesis filter bank (S); the multichannel inputs $u_{ST,m}[n]$ are the $P \leq (M-1)$ spatially strongly decorrelated components of $\mathbf{u}_{ST}[n]$ shown in Fig. 2.

design of a suitable prototype lowpass filter [12], and admit a very low computational cost [13].

The temporal prewhitening by filter banks can be exploited by two different structures:

- BEVD-Subband GSC (GSC-ST) performs strong spatial decorrelation first, followed by filter bank based temporal whitening;
- Subband-BEVD GSC (GSC-TS) uses a filter bank to prewhiten the array signals, and GSCs with strong spatial decorrelation such as shown in Fig. 2 are performed within each subband independently.

4.2 BEVD Subband GSC (GSC-ST) Beamformer

The first approach performs processing similar to the structure shown in Fig. 2 up to the output of $\mathbf{H}(z)$. Thereafter, each of the $P \leq (M-1)$ remaining strongly decorrelated subchannels with non-zero power is decomposed into K oversampled subbands. Within each of the K subbands, a multichannel adaptive filter (MCAF) with P inputs is operated in order to minimise the overall output $e[n]$. This configuration is depicted in Fig. 2.

Within each subband, the P inputs remain strongly decorrelated, while the support of the auto-correlation function of each input is shortened by approximately the decimation ratio $N < K$, leading to an additional temporal decorrelation. The power spectral matrix of the MCAF inputs therefore takes the same shape as (13) but has an approximately N times lower order.

Thus, spatio-temporal decorrelation is achieved through the GSC-ST structure. Reconstruction to the fullband signal can be performed by a synthesis filter bank (S) at the output of the MCAFs as shown in Fig. 3. This structure is expected to have faster convergence speed compared to the BEVD based GSC beamformer due to the additional temporal decorrelation and the reduced number of coefficients courtesy of only $P \leq (M-1)$ input signals to the adaptive process.

4.3 Subband BEVD GSC (GSC-TS) Beamformer

Reversing the order of decorrelation, a subband decomposition can be applied to each of the M array signals in $\mathbf{x}[n]$. Thereafter, in each of the resulting K subband signals a BEVD-GSC as outline in Fig. 2 is operated. This system setup is depicted in Fig. 4.

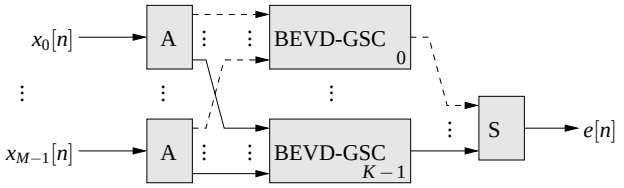

Figure 4: Subband-BEVD GSC (GSC-TS), whereby the array signals $x_m[n]$ are decomposed into K temporally decorrelated subbands. Within each subband, a BEVD-GSC according to Fig. 2 is operated, which implicitly performs a strong spatial decorrelation.

The subband decomposition performs a temporal decorrelation by reducing the support window of any correlation function by approximately a factor of N. As a result, the BEVD operates on a power spectral matrix with N times reduced order within each of the subbands. Therefore, SBR2 can be expected to converge faster and with lower order unitary matrices compared to the case of the BEVD-GSC outlined in Sec. 3. Within each subband, these unitary matrices achieve a strong spatial decorrelation. The power spectral matrix within each subband possesses a similar order and sparseness to the GSC-ST, and low power outputs can be omitted from further processing.

4.4 Overall Covariance Matrix

For the above cases of GSC-ST and GSC-TS, the overall covariance matrices across the TDLs of all adaptive processes differ in terms of their internal organisation, but share a common feature found in covariance matrices of subband adaptive filters. If $\mathbf{R}_{ij}(z)$ is the power spectral matrix defining the correlation between TDLs located in subbands i and j, then due to overlap between adjacent subbands, the matrix $\mathbf{R}$ describing all TDLs is tri-blockdiagonal with non-sparse corner elements [13],

$$\mathbf{R} = \begin{bmatrix} \mathbf{R}_{0,0} & \mathbf{R}_{0,1} & \mathbf{0} & \dots & \mathbf{0} & \mathbf{R}_{0,K-1} \\ \mathbf{R}_{1,0} & \mathbf{R}_{1,1} & \mathbf{R}_{1,2} & & \mathbf{0} & \mathbf{0} \\ \mathbf{0} & \mathbf{R}_{2,1} & \mathbf{R}_{2,2} & \ddots & & \vdots \\ \vdots & & \ddots & \ddots & \ddots & \mathbf{0} \\ \mathbf{0} & & & \ddots & \mathbf{R}_{K-2,K-2} & \mathbf{R}_{K-2,K-1} \\ \mathbf{R}_{K-1,0} & \mathbf{0} & \dots & \mathbf{0} & \mathbf{R}_{K-1,K-2} & \mathbf{R}_{K-1,K-1} \end{bmatrix}. \quad (14)$$

All off-block diagonal terms are due to redundancy in the oversampled system, and will disappear if the main block-diagonal correlation terms — on which they are dependent — are eliminated.

4.5 Complexity Considerations

Instead of applying SBR2 to the full covariance matrix, the GSC-TS calculates paraunitary matrices $\mathbf{H}_k(z)$, $k = 0 \cdots (K-1)$ based on individual subbands. The covariance matrices are based on decimated subband signals and will therefore have a smaller support, which results in both more accurate and faster computation. This also has the benefit of reducing the complexity of the SBR2 algorithm, since the number of iterations required to achieve the desired smallest value for off-diagonal elements is reduced.

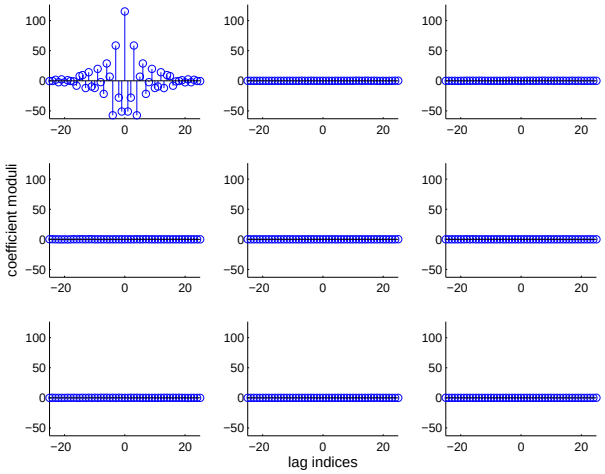

Figure 5: Polynomial covariance matrix after the application of SBR2. [Negative moduli — probably showing real part!]

Another difference between the GSC-ST and the GSC-TS beamformers is the number of analysis filter bank operations. In case of the GSC-TS, the number of analysis filter banks is linked to the number of sensor signals, M. For the GSC-ST, the count of analysis filter banks depends on the number of independent interferers, P. If the number of independent broadband interferers P is very small compared to the number of array sensors, this translates into lower complexity requirements for the GSC-ST beamformer compared to the GSC-TS beamformer.

5. SIMULATIONS AND RESULTS

The benefit of the proposed decorrelation for a broadband adaptive beamformer is demonstrated below in simulations. The simulated scenario contains a signal of interest which illuminates a $M = 4$ linear equispaced sensor array from broadside. The array is corrupted by an independent broadband interferer covering the spectral interval $\Omega \in [\frac{\pi}{8}, \frac{7\pi}{8}]$, with a signal to interference ratio of -35dB from an angle -20° measured against broadside.

The spatially decorrelated BEVD based GSC beamformer (GSC-S) requires an estimation of the polynomial covariance matrix $\mathbf{R}_{uu,\mathrm{S}}(z)$. The number of samples used to estimate this covariance matrix was chosen to be 1000, with the range of time delays set to $|\tau| \leq 25$. The polynomial covariance matrix $\mathbf{R}_{uu,\mathrm{ST}}(z)$ estimated from the signals $\mathbf{u}_{\mathrm{ST}}(z)$ is depicted in Fig. 5. As only one broadband interferer is present in the simulated scenario, all the output power is concentrated in the first diagonal element of $\mathbf{R}_{uu,\mathrm{ST}}(z)$ in Fig. 5.

The above BEVD based GSC beamformer (GSC-S) is benchmarked against the conventional time-domain CCD-GSC (GSC) setup without any prewhitening as well as a KLT-based GSC beamformer (KLT). All three beamformers operate using filters with $L = 140$ coefficients for the adaptation process. The CCD-GSC (GSC) beamformer was further enhanced by the introduction of temporal decorrelation through subband decomposition. This subband CCD-GSC (GSC-T) structure utilises a prototype filter of length $L_p = 448$ to decompose the received data into $K = 16$ subband signals decimated by $N = 14$ characterised in [6]. Due to the N times increased sampling period, a reduced TDL of

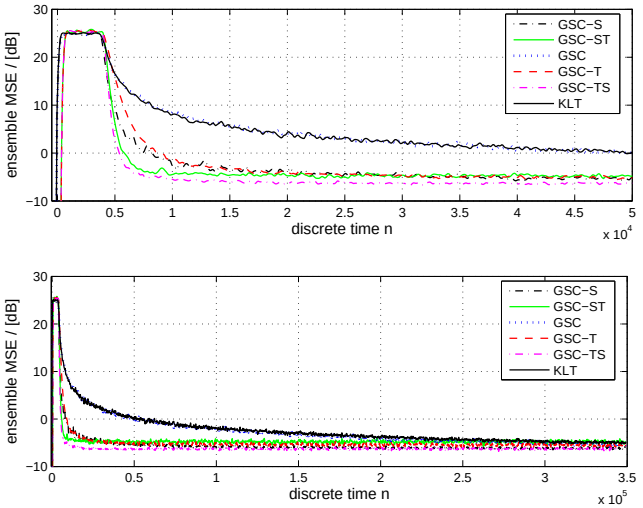

Figure 6: Learning curves for the various GSC implementations demonstrating (top) short term and (bottom) long term convergence behaviour: BEVD-GSC (here labelled GSC-S) with strong spatial decorrelation only; GSC-T with temporal decorrelation by means of a subband approach; GSC-ST by means of BEVD and subband decomposition; GSC-TS which performs subband decomposition prior to a strong spatial decorrelation; and (KLT) the GSC beamformer with decorrelation by a KLT.

length $L/N = 10$ filter coefficients has been applied for each subband. For this simulation scenario, a total of $M = 4$ analysis filter banks are required for subband decomposition.

The same subband approach was also incorporated into GSC-ST and GSC-TS beamformers to provide both strong spatial decorrelation as well as temporal decorrelation. Two different methods were explored for this integration. For the GSC-ST, a subband decomposition is performed on the $P = 1$ signal — the only signal carrying power as characterised the polynomial covariance matrix in Fig. 5 — and on the desired signal. The GSC-TS approach requires $M = 4$ analysis filter bank operations, followed by a BEVD calculation in each subband.

Using an NLMS adaptive algorithm to adjust the adaptive filter coefficients, the step sizes were chosen empirically for each of the beamformers discussed above to achieve approximately the same steady state mean squared error (MSE) across the various simulations. The performance in term of residual MSE, i.e. the beamformer output minus the signal of interest, over an ensemble of 50 simulations is shown in Fig. 6. Results indicate that the BEVD beamformer achieves better convergence speed compared to the CCD-GSC structure. The two beamformers which utilise both temporal and spatial decorrelation (GSC-ST and GSC-TS) outperform the remaining beamformers that only contain a decorrelation in maximally one dimension. The GSC-TS, which performs subband processing prior to the BEVD operation, converges slight faster due to better diagonalisation of the covariance matrix in the spatial domain as compared to the GSC-ST structure. The KLT beamformer proofs to be ineffective in our simulation scenario with convergence rate comparable to the time domain CCD-GSC beamformer, since the decorrelation is not accompanied by a power normalisation [4].

6. CONCLUSIONS

This paper has addressed a number of decorrelation approaches, in both space and time, to decorrelate the inputs to n adaptive beamformer, for which we have exemplarily used the GSC. We have shown that recently developed broadband EVD can help to improve the convergence speed with respect to standard implementations as well as a KLT implementation without power normalisation. The BEVD approach can be complemented by a spatial decorrelation by means of subband processing, for which additional benefits in terms of convergence speed were demonstrated in simulations. We have suggested two approaches, which differ in the order in which temporal (T) and spatial (S) decorrelations are imposed, and for which slight and scenario-dependent tradeoffs between complexity and convergence speed exist.

REFERENCES

[1] S. Haykin, *Adaptive Filter Theory*, Prentice Hall, Englewood Cliffs, 2nd edition, 1991.

[2] L. Ljung and T. Soderstrom, *Theory and Practice of Recursive Identification*, MIT Press, 1987.

[3] B. Widrow and S.D. Stearns, *Adaptive Signal Processing*, Prentice Hall, 1985.

[4] F. Beaufays, "Transform-domain adaptive filters: an analytical approach," *IEEE Trans. Sig. Proc.*,43(2):422–431, Feb. 1995.

[5] J.G. McWhirter, P.D. Baxter, T. Cooper, S. Redif, and J. Foster, "An EVD Algorithm for Para-Hermitian Polynomial Matrices," *IEEE Trans. Sig. Proc.*, 55(5):2158–2169, May 2007.

[6] S. Weiss. R.W. Stewart, M. Schabert, I.K. Proudler and M.W. Hoffman, "An Efficient Scheme for Broadband Adaptive Beamforming," *Asilomar Conf Signals, Systems, Computers*, Pacific Grove, 1:496–500, Nov. 1999.

[7] S. Weiss, A. Stenger, R.W. Stewart and R. Rabenstein, "Steady-State Performance Limitations of Subband Adaptive Filters," *IEEE Trans. Signal Proc.*, 49(9):1982–1991, Sept. 2001.

[8] O.L. Frost, III, "An algorithm for linearly constrained adaptive array processing," *Proc. IEEE*, 60(8):926–935, Aug. 1972.

[9] L.J. Griffiths and C.W. Jim, "An alternative approach to linearly constrained adaptive beamforming," *IEEE Trans. Antennas and Prop.*, 30(1):27–34, Jan. 1982.

[10] W. Kellermann, "Analysis and design of multirate systems for cancellation of acoustical echoes," in *ICASSP*, New York, 5:2570–2573, Apr. 1988.

[11] A. Gilloire and M. Vetterli, "Adaptive filtering in subbands with critical sampling: Analysis, experiments and applications to acoustic echo cancelation," *IEEE Trans. Sig. Proc.*, 40(8):1862–1875, Aug. 1992.

[12] M. Harteneck, S. Weiss, and R.W. Stewart, "Design of near perfect reconstruction oversampled filter banks for subband adaptive filters," *IEEE Trans. Circuits & Systems II*, 46(8):1081–1086, Aug. 1999.

[13] S. Weiss and I.K. Proudler, "Comparing Efficient Broadband Beamforming Architectures and Their Performance Trade-Offs," *14th Int. Conf. DSP*, Santorini, Greece, 1:417–422,July 2002.